

# SCIPIO – Validation of ATSR-2 and AATSR with SISTeR

Tim Nightingale

*Space Science and Technology Department, Rutherford Appleton Laboratory,  
Chilton, Didcot, Oxon OX11 0QX, England (email: [t.j.nightingale@rl.ac.uk](mailto:t.j.nightingale@rl.ac.uk))*

## Abstract

A SISTeR validation radiometer was deployed on the RRS Charles Darwin in June and July 2002 in the Indian Ocean as a part of the ENVISAT AATSR validation effort. End-of-life validation data were also collected for the ERS-2 ATSR-2 instrument. Skin SSTs were collected under a total of seventeen ENVISAT and ERS-2 overpasses. Owing to the lack of processed early-mission AATSR data, no AATSR validations have yet been made. ATSR-2 validations have been complicated by the degraded attitude control of the ERS-2 platform. Attitude correction files derived from the ERS-2 scatterometer have been incorporated into an ATSR-2 test processor. Significant geolocation errors are still present, particularly in the ATSR-2 forward view, but a preliminary validation has been attempted. Most differences between ATSR-2 and SISTeR are less than 0.3K.

## Introduction

The Scanning Infrared Sea surface Temperature Radiometer (SISTeR) from the Rutherford Appleton Laboratory (RAL) is a compact, self-calibrating filter radiometer designed to measure the skin temperature of the sea surface. A SISTeR was deployed on the RRS Charles Darwin as a part of the SCIPIO cruise with support from an EO enabling grant from the NERC for the beginning-of-life validation of the AATSR sea surface temperature sensor on the ESA ENVISAT satellite and the end-of-life validation of the ATSR-2 sensor on ERS-2. The cruise took place in the Indian Ocean, between the Seychelles and Mauritius, from the 1<sup>st</sup> June to the 11<sup>th</sup> July 2002.

## The SISTeR Instrument

A SISTeR was mounted on the handrails on the port quarter of the Darwin's foremast platform, facing outwards over the bow about 45° from the centre line. The SISTeR scan mirror was stepped out from the ship at small angular increments and the first clear view to the sea was identified at approximately 20° from nadir. A sea view at 25° was chosen for the standard scanning sequence, along with sky views at 50°, 25° and 0° from zenith. The views contained multiple radiance samples, each integrated for 0.8s. Skin SSTs were calculated from the sea view, with small corrections for reflected sky radiance from the 25° sky view<sup>1</sup>.

The SISTeR calibration was checked repeatedly against a CASOTS portable black body<sup>2</sup>, both before shipping and aboard the Darwin before, during and after the cruise (Figures 1 and 2). The CASOTS black body consists of a thin-walled copper cavity immersed in a water bath. The bath temperature was monitored with a Thermometrics AS125 thermistor, S/N 2228 and a Hart Scientific 1504 bridge S/N A14282. The combined accuracy of the thermistor and bridge was approximately 3mK at room temperature. The water in the CASOTS water bath was circulated with a 50W immersible pump, which doubled as a water heater, giving a temperature rise of approximately 3K every hour. The initial deviation of the brightness temperature recorded by the SISTeR from

the thermometric temperature of the water bath was approximately 10mK near to ambient temperature, with a slope of  $-1.5\text{mK/K}$  over the measurement range. Measurement noise on a 0.8s sample increased slightly through the cruise from an initial 30mK or so as the optical surfaces degraded, but the calibration result was reproduced to within the experimental accuracy on each calibration check. The radiometric error attributable to SISTeR in its normal operating region (ambient deviation of  $-5\text{K}$  to  $0\text{K}$  in Figures 1 and 2) was estimated to be less than 20mK.

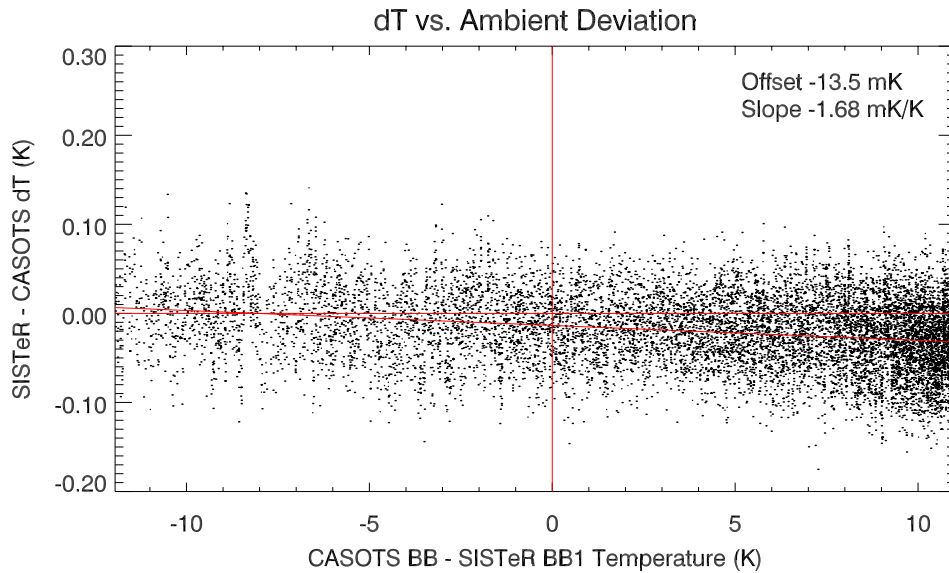


**Figure 1** Calibration of SISTeR against a CASOTS black body at RAL on the 8<sup>th</sup> May 2002, just prior to shipping. The SISTeR ambient black body, BB1, was operated at approximately 26°C during these measurements.

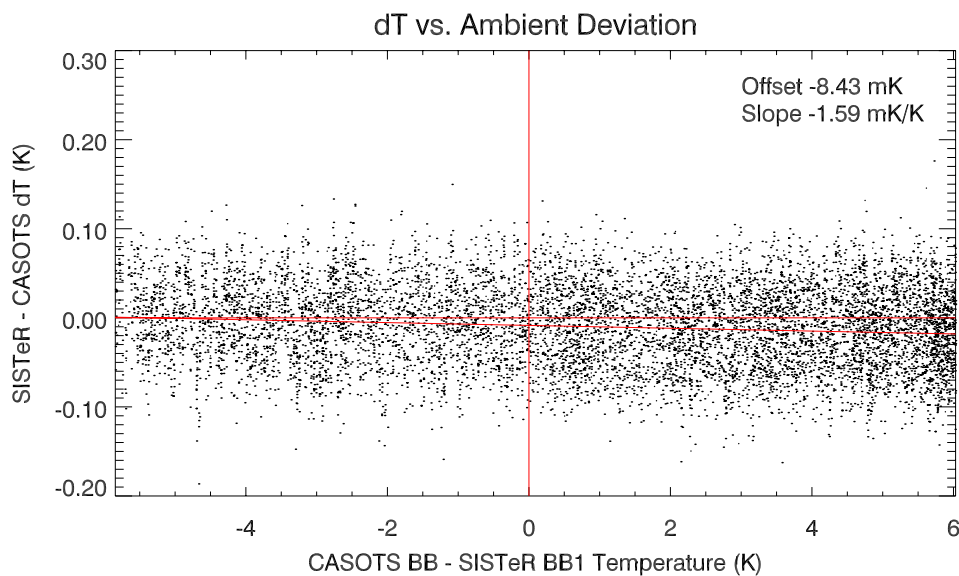


**Figure 2** Calibration of SISTeR against a CASOTS black body on board the RRS Charles Darwin on the 10<sup>th</sup> July 2002, just prior to return. The ambient black body, BB1, was operated at approximately 27°C during these measurements.

## Methodology

During the cruise, prospective ATSR-2 and AATSR overpasses were identified from time-tagged charts of the instrument swaths covering the immediate area in which the Charles Darwin was operating. The charts were interpolated from the ERS-2/ENVISAT reference orbit with an IDL program. Small modifications could be made to the cruise track to correct possible “near misses”, but in general the information was used to plan activities around the overpass time.

After the cruise, overpass points were refined to an “exact” time and position by considering the time-varying unit vectors  $\mathbf{n}_{\text{ship}}$  and  $\mathbf{n}_{\text{sat}}$ , pointing respectively from the earth’s centre to the Charles Darwin and to the satellites, ERS-2 or ENVISAT. The angle  $\theta$  between these vectors is at a minimum at the point of closest approach between the ship and the sub-satellite point.  $\theta$  is simply related to the dot product of the two vectors

$$\mathbf{n}_{\text{ship}} \cdot \mathbf{n}_{\text{sat}} = \cos \theta$$

so the overpass point can be found by searching for local maxima of the dot product  $\mathbf{n}_{\text{ship}} \cdot \mathbf{n}_{\text{sat}}$ . IDL code was written to perform a coarse search for local maxima, which were then refined by Newton-Rapheson iteration.  $\mathbf{n}_{\text{ship}}$  was derived from the ship’s GPS log and  $\mathbf{n}_{\text{sat}}$  either from the satellite reference orbit, from two-line elements or from the ATSR products themselves, once they had been generated. As the sub-satellite point moves far faster than the ship, the direction of closest approach is very nearly perpendicular to the satellite track. This allows a simple early test for viable overpasses: When the surface distance  $R_{\text{earth}} \theta$  is less than half of the ATSR swath width, or 256km, the point of closest approach will fall within the ATSR product.

## The Validation Data Set

The SISTeR was operated for about half of the total cruise time, starting a couple of hours after leaving the Seychelles on the morning of the 1<sup>st</sup> June and finishing early on the morning of the 10<sup>th</sup> July, a day before making port in Mauritius. Skin sea surface temperatures varied between approximately 24°C and 28°C (Figure 3). Poor weather limited observations below approximately 10°S. Scattered cloud was generally present although there were sometimes clear skies, especially at night over the northern part of the cruise track.

Using ERS-2 and ENVISAT sub-satellite tracks propagated from reference orbits, ATSR-2 and AATSR product requests were generated for all overpasses that passed the half-swath test (Tables 1 and 2). Those for ATSR-2 were subsequently updated with navigation data from the products themselves. The cruise track coincided with the AATSR swath on seventeen occasions (Table 1, Figure 4), always near to 10.00am or 10.00pm local time, and with the ATSR-2 swath approximately half an hour earlier (Table 2). Of these, four or five fell within the clear intervals and were prospects for validations of the ATSR instruments. Balloon GPS sondes were also released for the 6am and 6pm UTC synoptic times that most closely coincided with the overpasses.

At the time of writing, AATSR Level 1 and 2 products for the CD141 cruise were not available from ESA. GBT and GSST images for four ATSR-2 overpasses (4, 6, 8 and 16) have been processed to Levels 1 and 2 on a test

Overpass	Julian Day UTC	Time UTC	Latitude	Longitude	Across track Position (km)	Comments
1	152	06:36:28	4°33.14'S	55°40.23'E	182	
2	153	18:36:56	4°17.99'S	56°31.87'E	220	Cloud
3	155	06:42:12	5°14.08'S	57°17.29'E	164	Cloud
4	156	18:41:42	7°12.98'S	58°19.62'E	59	
5	159	06:17:14	8°00.01'S	61°23.68'E	24	Cloud
6	160	18:15:43	8°00.14'S	64°00.89'E	42	
7	163	05:52:29	11°27.12'S	65°19.49'E	211	Cloud
8	163	18:20:10	12°18.28'S	65°19.77'E	148	30kt winds
9	166	05:59:37	16°29.26'S	63°26.77'E	132	Cloud
10	166	18:24:31	17°52.79'S	62°43.02'E	110	Rain
11	169	06:06:14	19°39.36'S	61°58.71'E	56	Cloud
12	169	18:29:44	19°45.00'S	61°55.48'E	88	Rain
13	175	06:17:30	18°36.87'S	58°25.16'E	152	Cloud
14	175	18:41:40	18°00.13'S	59°42.06'E	21	Cloud
15	178	06:21:47	14°12.79'S	61°56.18'E	258	Cloud
16	182	18:24:02	9°25.03'S	61°18.96'E	134	
17	184	06:31:39	8°00.77'S	58°10.50'E	17	Cloud

**Table 1** ATSR-2 overpass analysis for CD141. The time and ship's position at overpass is listed, along with the distance of the overpass from the centre of the ATSR-2 swath and a note on the conditions at overpass.

Overpass	Julian Day UTC	Time UTC	Latitude	Longitude	Across Track Position (km)	Comments
1	152	06:07:59	4°34.12'S	55°36.51'E	189	
2	153	18:08:28	4°17.81'S	56°31.98'E	220	Cloud
3	155	06:13:44	5°14.07'S	57°17.28'E	165	Cloud
4	156	18:13:14	7°12.80'S	58°18.35'E	58	
5	159	05:48:45	8°00.02'S	61°19.86'E	31	Cloud
6	160	17:47:12	8°00.04'S	64°00.79'E	43	AATSR off
7	163	05:23:56	11°23.91'S	65°19.81'E	212	Cloud
8	163	17:51:38	12°18.29'S	65°19.81'E	147	30kt winds
9	166	05:31:04	16°29.21'S	63°26.86'E	132	Cloud
10	166	17:55:58	17°49.54'S	62°45.08'E	107	Rain
11	169	05:37:39	19°35.70'S	61°59.89'E	56	Cloud
12	169	18:01:10	19°44.99'S	61°55.44'E	90	Rain
13	175	05:48:56	18°37.85'S	58°23.89'E	155	Cloud
14	175	18:13:06	18°00.00'S	59°42.03'E	19	Cloud
15	178	05:53:13	14°12.81'S	61°55.91'E	257	Cloud
16	182	17:55:28	9°26.06'S	61°24.08'E	126	
17	184	06:03:05	7°59.96'S	58°11.94'E	18	Cloud

**Table 2** AATSR overpass analysis for CD141. The time and ship's position at overpass is listed, along with the distance of the overpass from the centre of the AATSR swath and a note on the conditions at overpass.

processor (T360) at RAL, incorporating attitude correction data derived from the ERS-2 scatterometer. These are illustrated in Figures 5 – 8. There is an along track difference in registration of approximately 40km between the instrumental views for overpass 4. Across-track agreement is to approximately 5km. For overpass 6, the along track difference is of order 20km, with little discernable across track displacement. Overpass 8 appears quite well registered, with displacements of order 5km in both the along and across track directions. The views from overpass 16 are displaced by a similar amount.

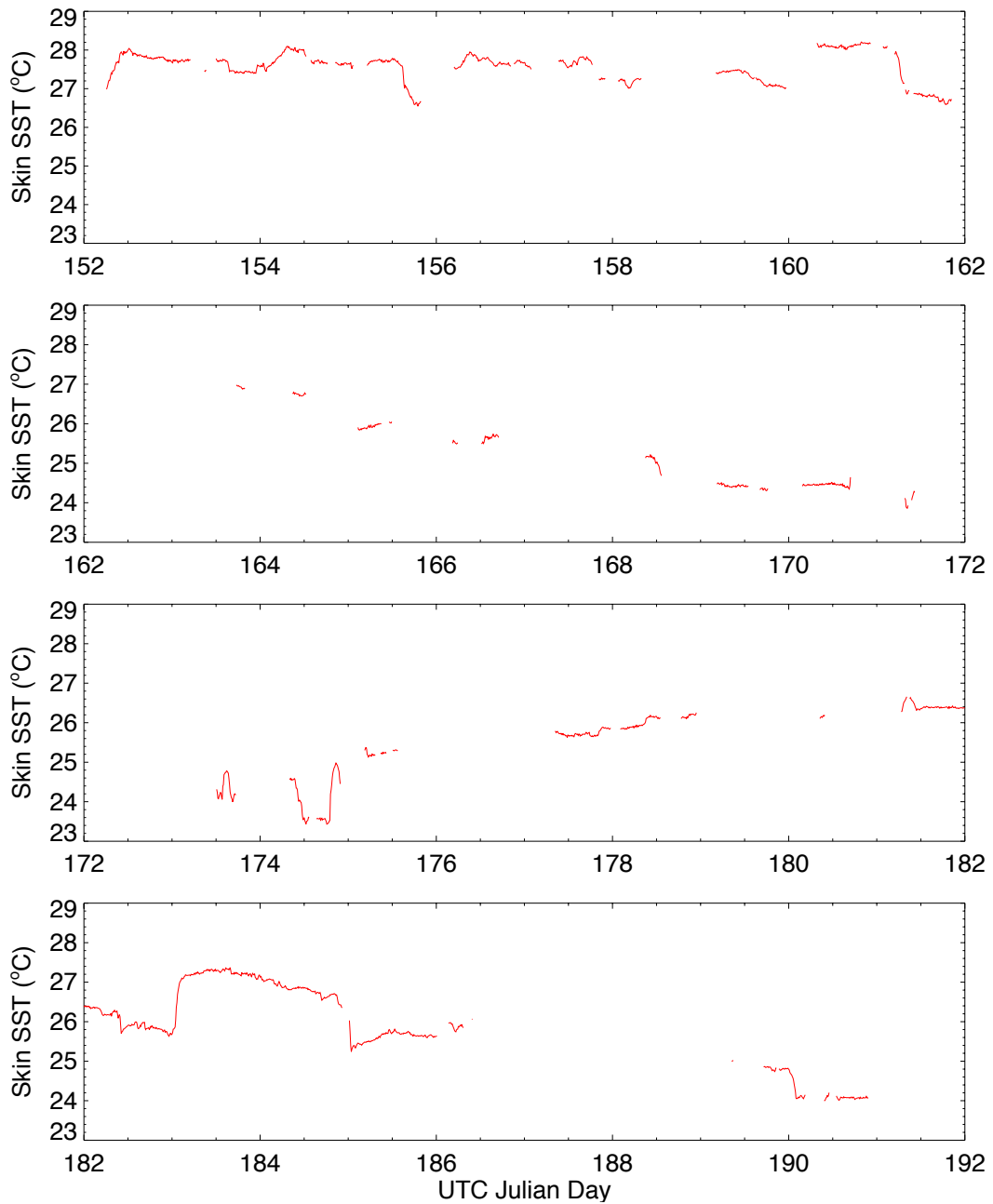


**Figure 3** Summary of SISTeR skin sea surface temperatures for CD141.

Given the large amounts of nearby cloud, these displacements introduce significant problems in the calculation of dual view SSTs. Both overpasses 4 and 6 could well yield more substantial overpass data, but the along track misalignment causes large numbers of pixels to be masked in one or other view, when this would not be the case for better registered data. Some improvement may be possible with relative naked eye or corollary alignments of the forward and nadir views. The cloud base was generally less than 1,000m, so the cloud outlines should give a reasonable guide.

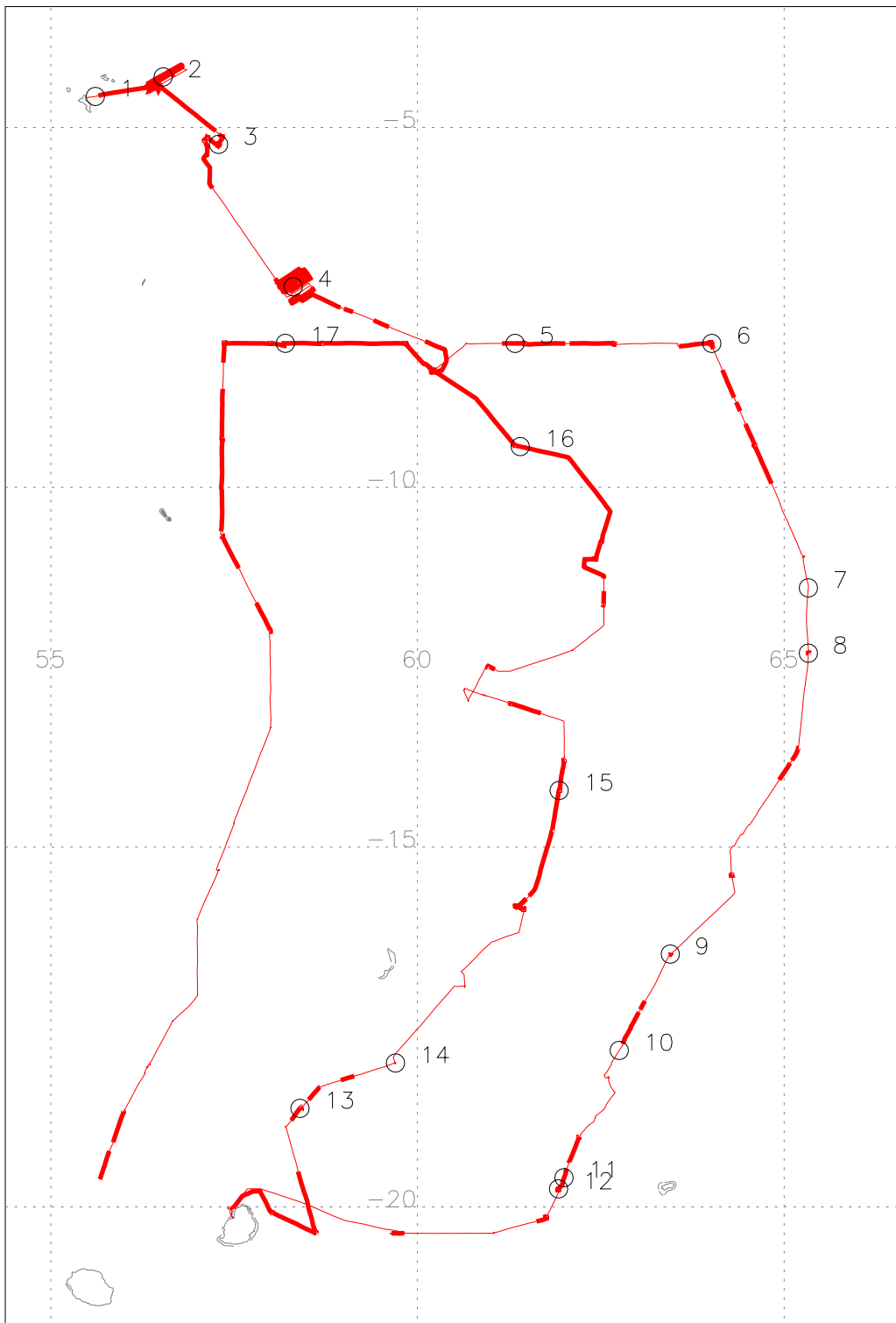


**Figure 4** The cruise track for CD141, showing the availability of SISTeR data and the positions of the seventeen ATSR-2 and AATSR overpasses (details in Tables 1 and 2).

## ATSR-2 Validation Results

The SISTeR skin SSTs at overpass (Table 3) in general correspond well to the various averages of ATSR-2 SST (Tables 4 and 5), to 0.3K or better in most cases. The mean deviations of the ATSR-2 50km nadir-only and dual view SSTs from the SISTeR 1 hour SSTs are +0.09K and \_0.03K respectively. The SISTeR reported steady SST values and consistently low standard deviations across all of the averaging intervals for these points, so large area, long period comparisons may be permissible. The ATSR-2 SST standard deviations are, however, quite high for the dual view averages, suggesting that misalignment is a significant problem.

Overpass	±1 min	±2 mins	±5 mins	±10 mins	±20 mins	±60 mins
<b>SST mean</b>						
4	300.78K	300.79K	300.79K	300.79K	300.79K	300.79K
6	301.31K	301.30K	301.30K	301.29K	301.29K	301.27K
8	300.11K	300.11K	300.11K	300.10K	300.10K	300.09K
16	299.02K	299.02K	299.02K	299.02K	299.02K	299.00K
<b>SST standard deviation</b>						
4	0.03K	0.03K	0.03K	0.04K	0.04K	0.03K
6	0.03K	0.03K	0.03K	0.04K	0.04K	0.04K
8	0.04K	0.04K	0.04K	0.04K	0.04K	0.05K
16	0.03K	0.03K	0.03K	0.03K	0.04K	0.04K
<b>Number of samples</b>						
4	70	140	346	672	1322	4000
6	64	128	320	660	1344	4002
8	70	140	346	672	1321	3456
16	70	140	350	672	1321	4000

**Table 3** SISTeR mean skin sea surface temperatures for overpasses 4, 6, 8 and 16, averaged over bins extending 1, 2, 5, 10, 20 and 60 minutes either side of the overpass time, with the number and standard deviation of SISTeR samples for each bin.

Overpass	1 km	2 km	5 km	10 km	20 km	50 km
<b>SST mean</b>						
4	–	–	–	–	300.81K	300.82K
6	–	–	301.30K	301.36K	301.24K	301.15K
8	–	–	–	300.26K	300.41K	300.36K
16	–	–	–	–	299.45K	299.16K
<b>SST standard deviation</b>						
4	–	–	–	–	0.19K	0.34K
6	–	–	0.20K	0.18K	0.26K	0.32K
8	–	–	–	0.25K	0.13K	0.14K
16	–	–	–	–	0.12K	0.34K
<b>Number of pixels</b>						
4	–	–	–	–	76	1097
6	–	–	10	57	155	2066
8	–	–	–	11	425	2326
16	–	–	–	–	15	200

**Table 4** ATSR-2 nadir-only mean skin sea surface temperatures, masked with the nadir cloud flag, for overpasses 4, 6, 8 and 16, averaged over bins extending 1, 2, 5, 10, 20 and 50 kilometres from the overpass point, with the number and standard deviation of ATSR-2 pixels for each bin.

Overpass	1 km	2 km	5 km	10 km	20 km	50 km
<b>SST mean</b>						
4	–	–	–	–	300.58K	300.76K
6	–	–	300.51K	301.16K	301.29K	301.07K
8	–	–	–	–	300.33K	300.21K
16	–	–	–	–	–	299.01K
<b>SST standard deviation</b>						
4	–	–	–	–	0.46K	0.71K
6	–	–	0.26K	0.42K	0.53K	0.49K
8	–	–	–	–	0.33K	0.29K
16	–	–	–	–	–	0.54K
<b>Number of pixels</b>						
4	–	–	–	–	61	74
6	–	–	2	48	127	1967
8	–	–	–	–	294	2113
16	–	–	–	–	–	58

**Table 5** ATSR-2 dual view mean skin sea surface temperatures, masked with the nadir and forward cloud flags, for overpasses 4, 6, 8 and 16, averaged over bins extending 1, 2, 5, 10, 20 and 50 kilometres from the overpass point, with the number and standard deviation of ATSR-2 pixels for each bin.

### Acknowledgements

The author would like to thank the officers and crew of the RRS Charles Darwin for their assistance during the cruise. This work was funded by an EO enabling grant from the UK NERC and was carried out in collaboration with the University of Leicester.

### References

1. C.J. Donlon and T.J. Nightingale: Effect of atmospheric radiance errors in radiometric sea-surface skin temperature measurements. *Applied Optics*, **39**, 2387-2392 (2000).
2. C.J. Donlon, T. Nightingale, L. Fielder, G. Fisher, D. Baldwin and I.S. Robinson: The calibration and intercalibration of sea-going infrared radiometer systems using a low cost blackbody cavity. *J. Atmos. Oceanic Technol.*, **16**, 1183-1197 (1999).

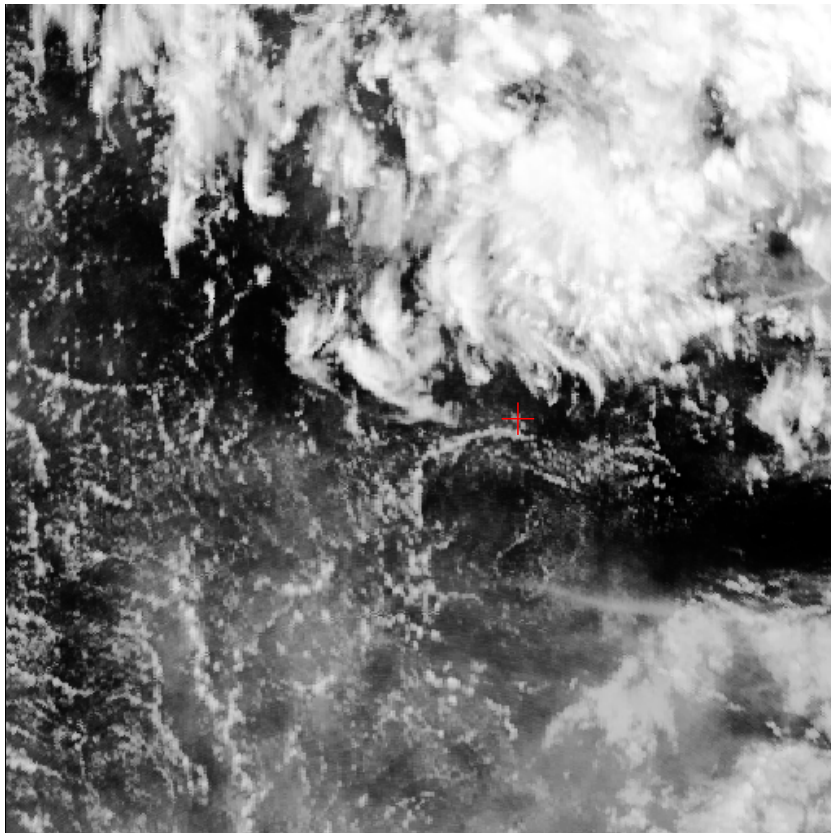
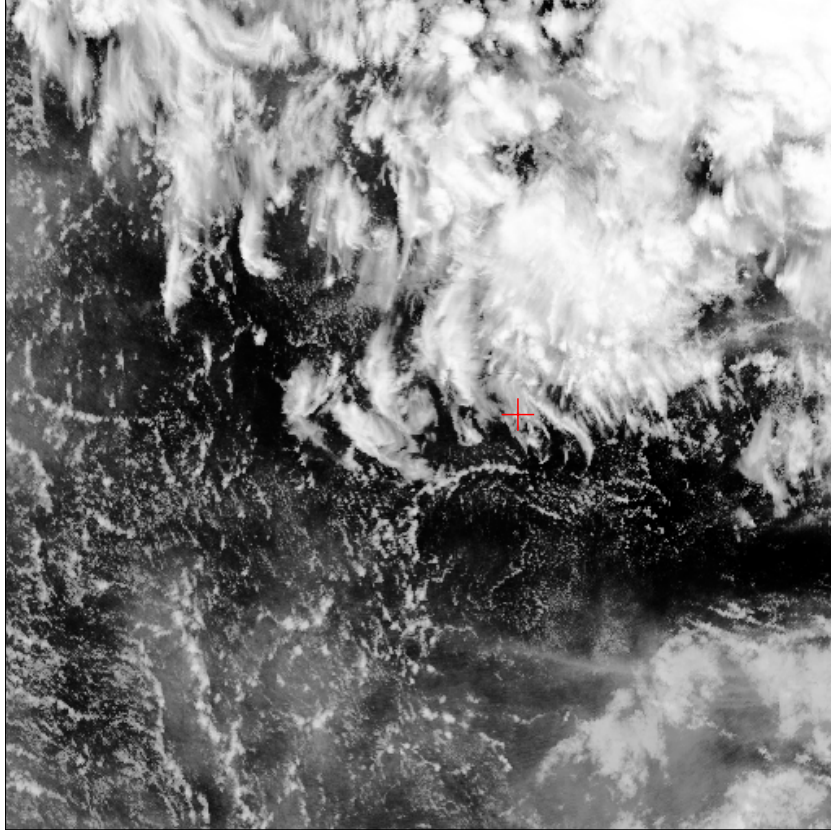


**Figure 5** ATSR-2 nadir (top) and forward (bottom) 11 $\mu$ m brightness temperature images for overpass 4 on the evening of day 156 (5<sup>th</sup> June, 2002). The position of the RRS Charles Darwin is shown with a red cross.



**Figure 6** ATSR-2 nadir (top) and forward (bottom)  $11\mu\text{m}$  brightness temperature images for overpass 6 on the evening of day 160 (9<sup>th</sup> June, 2002). The position of the RRS Charles Darwin is shown with a red cross.

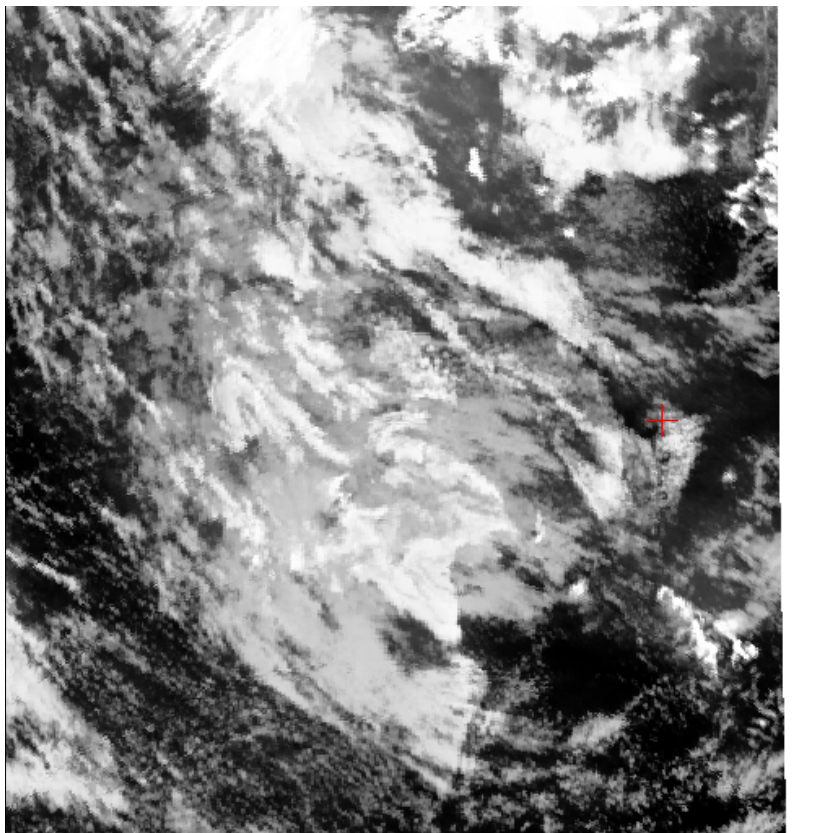
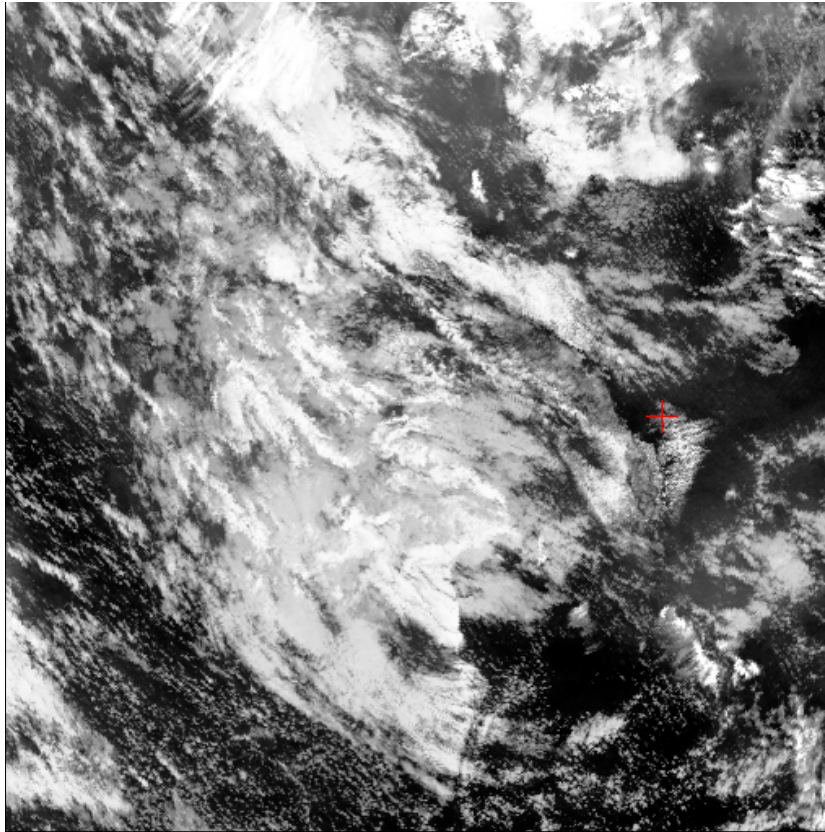


**Figure 7** ATSR-2 nadir (top) and forward (bottom)  $11\mu\text{m}$  brightness temperature images for overpass 8 on the evening of day 163 (12<sup>th</sup> June, 2002). The position of the RRS Charles Darwin is shown with a red cross.

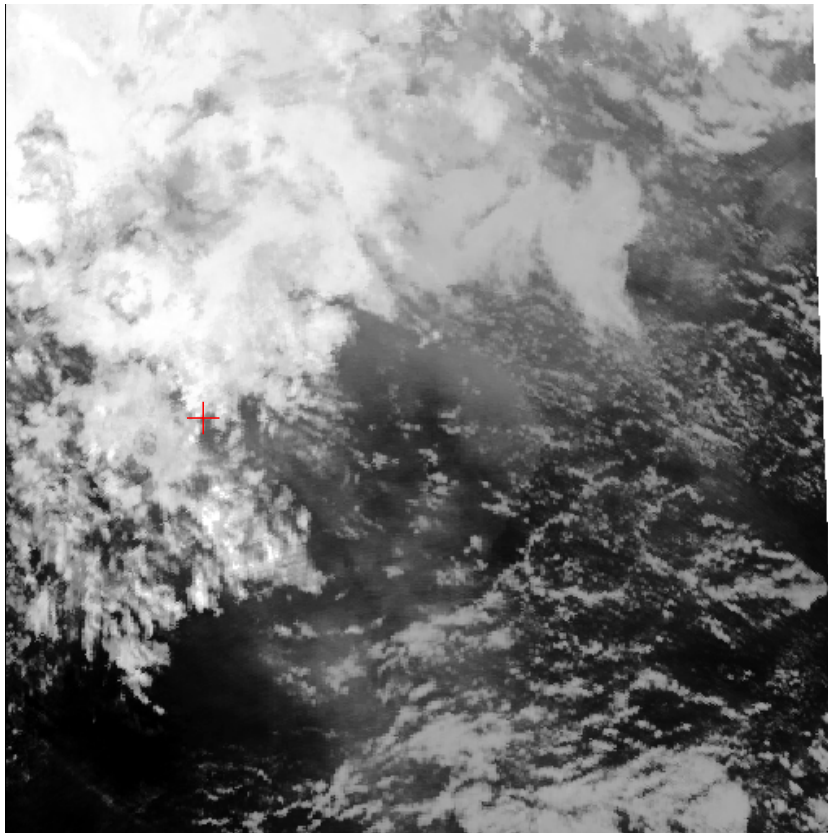
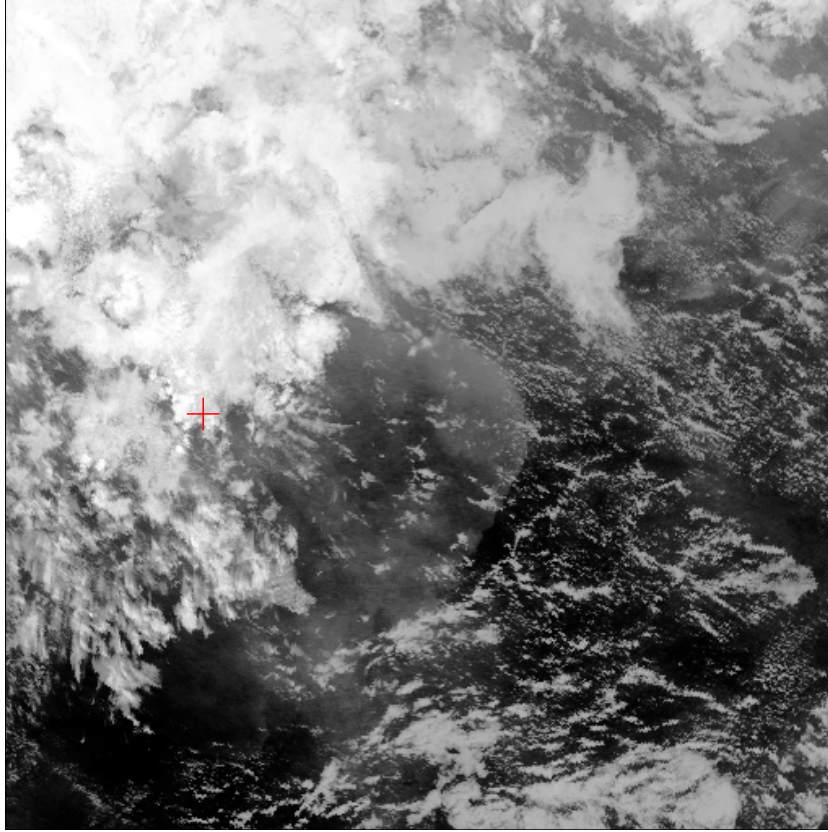


**Figure 8** ATSR-2 nadir (top) and forward (bottom)  $11\mu\text{m}$  brightness temperature images for overpass 16 on the evening of day 182 (1st July, 2002). The position of the RRS Charles Darwin is shown with a red cross.